Volume 5 JUNE, 1934 Number 6

PHYSICS

A Journal of General and Applied Physics

X-Ray Crystal Measurements of Nickel at High Temperatures

WILLIAM P. JESSE, *Research Laboratory, General Electric Company, Schenectady, New York*

(Received April 2, 1934)

X-ray powder photographs have been made of an electrically heated nickel ribbon sealed into a thin-walled glass bulb. X-ray measurements extending from 450 to 1200°C showed no new high temperature crystal form of nickel. The thermal expansion of the face-centered cubic lattice, present throughout the range investigated, is in agreement with macroscopic thermal expansion data.

OF the periodic group of elements, iron, nickel, cobalt, both iron[1] and cobalt[2] have two high temperature crystal forms in addition to the one usually occurring at ordinary temperatures. It would seem likely therefore that nickel would have another crystal form in addition to the usual face-centered cubic one. A hexagonal close-packed lattice has been reported by G. P. Thomson[3] as the result of electron diffraction measurements on a thin film of nickel sputtered on rocksalt in an atmosphere of argon. Attempts to obtain this form, or any other than the cubic form, by rapid quenching from high temperatures of nickel bars have not been successful. Such negative results in quenched bars do not eliminate the possibility of a high temperature crystal form since such a form may well revert to the low temperature form during even the most rapid quenching. Such is the case with pure iron.

Recently a simple technique has been developed by the writer whereby x-ray powder diffraction photographs of specimens in a vacuum or in an inert gas may readily be obtained. It seemed worth while therefore to make some measurements of a pure nickel ribbon at varying high temperatures to determine whether a second crystal form could be found and, in any event, to determine the dimensions of the crystal lattice at such temperatures. It seemed also that the method might be of value for other measurements of a similar character in case it proved itself capable of giving satisfactory results.

EXPERIMENTAL PROCEDURE

The x-ray measurements were made on a ribbon of very pure nickel bent into a hairpin filament and sealed into a thin-walled lime glass bulb filled with argon. The bulb was 2.5 centimeters in diameter and the walls were less than 0.01 cm thick. It was found that quite satisfactory powder photographs with copper radiation could be taken of a metal ribbon enclosed in such a bulb. The nickel used was formed by reducing pure nickel oxide in hydrogen, the resulting powder being then melted into an ingot in a vacuum furnace. This ingot was then swaged and drawn into a wire 10 mils (0.025 cm) in diameter and the latter was finally rolled out into a ribbon of dimensions $1\frac{1}{2} \times 44$ mils (0.004×0.11 cm). All annealing during the process of drawing was done in a vacuum furnace. A

[1] A. Westgren and A. E. Lindh, Zeits. f. physik. Chemie **98**, 181 (1921).
[2] S. B. Hendricks, M. E. Jefferson and J. F. Shultz, Zeits. f. Kristallographie **73**, 376 (1930).
[3] G. P. Thomson, Proc. Roy. Soc. **A125**, 358 (1929).

spectroscopic analysis of the nickel showed only a trace of cobalt and a trace of silicon as impurities.

The nickel filament was mounted in the thin-walled bulb and the latter was baked, after which the filament was degassed by heating and the bulb then filled with argon and sealed off. The x-ray measurements were made with the bulb mounted on an ordinary crystal spectrometer which was fitted with a precision camera of 7 cm diameter. The film was placed in the camera so that the entering beam passed through it as in the method of van Arkel.[4] The nickel filament was heated by passing a current through it from a heavy duty storage battery, the conditions of current and voltage being kept quite constant during each run. About a dozen photographs were taken of the glowing filament at temperatures ranging from 450 to 1200°C. The x-ray beam through the camera slits was directed at one arm of the hairpin filament and this arm was carefully centered in the camera by the use of a short focus telescope after the proper filament temperature had been attained for any given run. The bulb and filament were oscillated by means of the usual rocking cam, and care was taken that the second arm of the filament did not enter the path of the beam at any time during the oscillation to give spurious lines. The partial blocking off from the film of a small section of the diffracted rays by the second arm of the filament was of small consequence.

For filament temperatures above 800°C, temperature measurements were made with an optical pyrometer. Below 800°C, the temperatures were only approximately determined. Pyrometer temperatures were converted into true temperatures by making the proper corrections for the thermal emissivity of a bright nickel surface. The relation between brightness temperature ($\lambda = 0.665\mu$) and true temperature from the *International Critical Tables* was used.[5] No correction was made for the absorption due to the thin-walled bulb since experiment showed such a correction to be negligible. Although it is fully realized that pyrometer measurements of other than black bodies may be subject to large errors, it is believed that with the precautions taken in this case the final temperatures obtained are very close to the true temperatures.

Results

Measurements at room temperature

Widely differing values for the size of the unit cube for nickel at room temperatures are quoted from the literature in the *Strukturberichte*[6] of Ewald and Hermann. Such values for the length of the cube edge vary from 3.499A to 3.536A. It seems therefore worth while to record the result of a series of precision measurements made at room temperature with the very pure specimen of nickel available. After small corrections[4] were made for faulty centering and any possible change in the length of the film during development, the values obtained from three different specimens for the length of the cube edge of nickel at 20°C were, respectively, 3.517_9A, 3.518_4A, 3.517_2A. The mean 3.518 ± 0.001A is in good agreement with the value 3.519 ± 0.001A chosen in the *Strukturberichte* as the most probable value from the data available.

High temperature measurements

All the x-ray photographs of the hot nickel ribbon throughout the range of temperatures investigated (450 to 1200°C) gave lines corresponding to a face-centered cubic lattice. No lines corresponding to any other possible modification were observed on any of the photographs. One is therefore forced to the conclusion that, unlike iron and cobalt, nickel shows no structural lattice transformation within the region investigated, and that a face-centered cubic structure is characteristic of the metal throughout this temperature range. It seems probable therefore that the hexagonal crystal form observed by G. P. Thomson[3] cannot be obtained from thermal effects alone but probably is dependent for its existence upon the conditions of deposition of the sputtered film and possibly upon the base material upon which the nickel is sputtered.

As is to be expected, due to thermal expansion, the dimensions of the face-centered cubic nickel lattice were found to increase with temperature. The values obtained for the length of the cube edge of the observed face-centered structure are

[4] A. E. van Arkel, Zeits. f. Kristallographie **67**, 235 (1928).

[5] Int. Crit. Tab. **5**, 245.

[6] Ewald and Hermann, *Strukturberichte*.

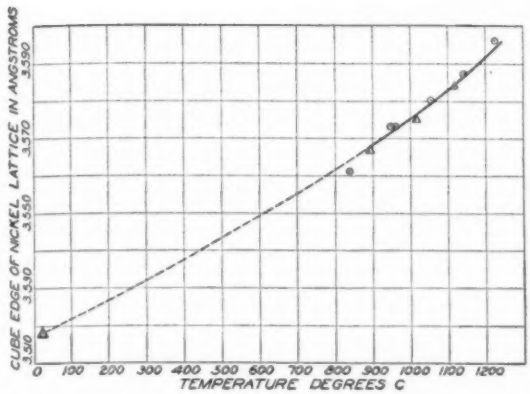

FIG. 1. Curve showing expansion of unit cube of nickel lattice with temperature. Full line from direct x-ray measurements, dotted line from calculations from thermal expansion data.

plotted in Fig. 1 against the corresponding corrected pyrometer temperatures between the temperatures 850 and 1200°C. Data from two different specimens are indicated by △ and ⊙, respectively. The resulting curve is indicated by the full line in the diagram. Average values obtained from the curve for the length of the cube edge at various temperatures are tabulated for convenience in Table I.

A comparison of the values obtained above with values computed from the usual thermal expansion data seems desirable since, for single crystals of bismuth,[7] discrepancies have been found between the macroscopic and the microscopic expansion data. No accurate results for the thermal expansion of nickel could be found covering the complete range 850 to 1200°C. Hidnert,[8] however, has carefully determined

[7] A. Goetz and R. C. Hergenrother, Phys. Rev. **40**, 643 (1932).

[8] Peter Hidnert, Bur. Standards J. Research, Tech. Paper **257**, 1306 (1930).

TABLE I. *Values of length of cube edge of nickel lattice at measured temperatures.*

Temperatures degrees C	Length of cube edge of nickel lattice in A	Length of cube edge calculated from thermal expansion data
20	3.518±0.001	
900	3.568±0.002	3.568
1000	3.575±0.002	
1100	3.583±0.002	
1200	3.592±0.002	

average expansion coefficients for a specimen of 99.94 percent pure nickel for a number of temperature ranges between the limits 25 and 900°C. Such data will serve for a calculation of the cube edge of the nickel lattice at temperatures up to 900°C, if we assume that the lattice expansion is exactly the same as the large scale expansion. The dotted curve in Fig. 1 is derived thus from Hidnert's data where the value of the cube edge at 20°C is taken as 3.518A. This curve is seen to be a smooth continuation of the full line curve based on direct x-ray measurements. The value of the length of the cube edge at 900°C calculated from Hidnert's average expansion coefficient for the full range 25–900°C is found to be 3.568A. (Table I.) This is just the value determined by x-ray measurements. It would seem therefore that within the limits of error of the measurements, the average expansion of the nickel lattice from 20 to 900°C as determined by direct x-ray measurements is the same as that calculated from macroscopic expansion data.

The writer wishes to extend his thanks to Mr. E. F. Hennelly of the General Electric Research Laboratory for furnishing the samples of nickel used and to Mr. E. T. Asp for assistance in obtaining some of the x-ray photographs.

The Charges on Droplets Produced by the Spraying of Liquids as Revealed by the Millikan Oil Drop Method

SEVILLE CHAPMAN,[1] *University of California*

(Received February 24, 1934)

THE electrification of liquids by spraying is a well-known phenomenon which has important industrial as well as purely scientific interest. One phase of the problem, the investigation of spray electrification of water, has been thoroughly studied by P. Lenard[2] and his pupils. His researches indicated that the phenomena of cataphoresis of gas bubbles, waterfall electricity, electrification from jets and atomization by impact and bubbling are all intimately connected with the surface conditions of liquids, involving the so-called electrical double layer of the surface, and any electrolytic ions contained therein.

According to Lenard and also to Coehn[3] this stratification is determined by surface tension and dielectric constant of the liquid. Accordingly, while water should show a most pronounced effect, substances of lower dielectric constant should also show the effect, though to a lesser degree. Studies of cataphoresis of gas bubbles seemed to indicate that the effect, while present in water, was not observable in liquids of lower dielectric constant. Dyk[4] found, in such liquids, that before marked cataphoresis of air bubbles occurred, the turbulence caused by ionic movements in the high fields set in, thereby making further study impossible. Spray electrification, however, is daily observed, even in such substances as pure hydrocarbons. Lenard and his pupils found that for water, the small droplets were negatively charged, while the larger drops were positively charged if ions were present; otherwise, they were neutral. In general, Bühl[5] confirms these findings, but Busse[6] found that some positively charged drops were produced in pure water, although not in such quantity as the negative drops.

As a quantitative method for a study of this spray electrification, it seemed that the Millikan oil drop method would give valuable information on the effect of drop size as related to charge.

For the purpose of this study, a conventional Millikan oil drop apparatus was employed, the droplets entering the condenser space by means of gravity through a hole in the upper plate. The condenser plates were separated by 0.8 cm. A potential from 2000 volts downward, could be applied to the plates. Light from a 1000 watt projection lamp, filtered with a $CuCl_2$ solution in a water cell, was used for illumination. The telescope had a 10 cm focal length and a magnification of 20 times. The droplets were produced by a brass atomizer of a conventional design, in which the liquid was drawn up through a fine brass tube and atomized by a high velocity stream of clean, filtered, compressed air issuing from a nozzle at right angles, pressures of 6–8 lbs./in.^{2} being used. The substances used, together with the purification resorted to, are listed below:

1. Ameroil, a pure, inert medicinal hydrocarbon, largely octane; taken from drugstore samples.
2. Nitrobenzene; highly purified for use in Kerr cells, as prepared by H. J. White in his study of Kerr cells. This was especially pure nitrobenzene, which was exceptionally free from ions.
3. Aniline; twice redistilled in air, using only the sharp middle fraction.
4. Glycerine; the water heated out of it and distilled in vacuum, only the middle fraction being used.
5. Ordinary distilled water.

Further substances were not tried, as it was difficult to find any of significantly different properties which would not evaporate too rapidly.

All measurements were made at atmospheric pressure and 20°C. With water, nitrobenzene and

[1] Introduced by Leonard B. Loeb.
[2] Lenard, Ann. d. Physik **47**, 463–524 (1915).
[3] Coehn, Ann. d. Physik **43**, 1048–1078 (1914).
[4] Dyk, Phys. Rev. **31**, 913 (1928).
[5] Bühl, Koll. Zeits. **59**, 346–353 (1932).
[6] Busse, Ann, d. Physik **76**, 493–533 (1925).

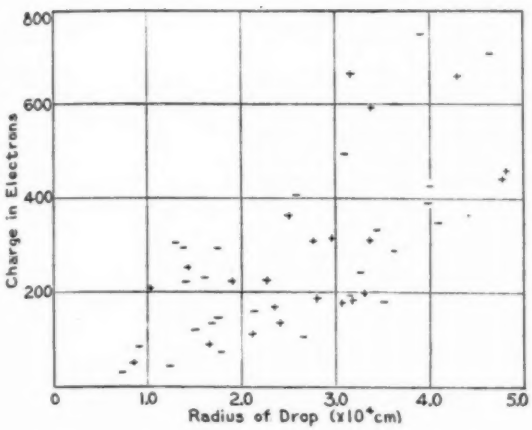

FIG. 1. Charge as a function of drop size in nitrobenzene.

aniline, considerable difficulty was encountered, due to the evaporation of the drops during measurements. This was only partially overcome by saturating the air inside the chamber with the vapor of the liquid.

The results obtained in the case of nitrobenzene are summarized in the graph of Fig. 1. In this graph, the drops, characterized as positive or negative by a + or − sign, are plotted with their charge in electrons against the radius of the drop in centimeters. It must be noted that, owing to evaporation, accurate values of the charge in exact multiples of the charge of the electron could not be obtained. Consequently, the values were computed to the nearest whole multiple of e. The values are good to about 15 percent.

It is seen at once that the charge varies in magnitude with drop size, being greater for the larger drops. This holds for all substances, except Ameroil, where all charges are uniformly low. It is to be emphasized that in this range of sizes no substance (including Ameroil) showed any correlation of drop size with sign of charge. Different substances, however, varied widely in the magnitude of the charge for approximately the same size of drops. The relation of the magnitude of the charge to dielectric constant and other properties of the substances are shown in Table I. For each substance in the table are given the dielectric constant, the surface tension, and the viscosity taken from standard tables; the radius of the smallest drops with their average charge, and the radius of the largest drops with their average charge.

The drop sizes were limited to relatively narrow ranges of size. This is due to a number of causes. The mass of the drops increases as the cube of their radii. Thus, for larger drops the short time of fall under gravity, and the necessity of sufficiently high charges to make them alter their speed, precluded measurements of very large drops. This was especially important in the case of Ameroil, where the charges per drop are small, but was of little significance in the cases of the polar liquids, which gave more highly charged drops. Measurements on small drops become impossible, owing to the violent Brownian, and slight convectional movements, and in the case of the more volatile liquids to the rapid evaporation of the drops. This latter factor made the results in water yield orders of magnitude only. These measurements were, however, important in showing that in this range of drop size, water behaved in a fashion similar to the other substances. It is very possible that the actual magnitudes of the charges on the water drops could have been greater than those on nitrobenzene, although this is not certain.

TABLE I. *Charge on drops as related to other liquid properties.*

Liquid	Dielectric constant	Surface tension in dynes/cm	Viscosity in dyne sec./cm²	Smallest Drops		Largest Drops	
				Radius in cm	Average charge in electrons	Radius in cm	Average charge in electrons
						$\times 10^{-4}$	
Ameroil	1.9	27.0	0.054	4.0×10^{-5}	2	1	2
Nitrobenzene	35.7	46.0	0.021	1.0×10^{-4}	150	4	800
Aniline	7.3	44.0	0.044	1.5×10^{-4}	100	5	450
Glycerine	56.2	65.2	0.083	5.0×10^{-5}	40	2.5	500
Water	80.0	72.8	0.010	1.5×10^{-4}	125	5	600

From the table it is seen that in the range of drop size used there is:

1. No preference for either sign of charge.
2. The larger drops of both signs of charge have the larger charges, and that the charge varies roughly in a linear fashion with drop size, except as previously noted in the case of Ameroil.
3. That there is a rough parallelism between dielectric constant and charge magnitude for drops of approximately the same size.
4. That although there appears to be no correlation with viscosity, a parallelism between drop size and surface tension exists which is, however, difficult to differentiate from that with dielectric constant.

There was only one substance, Ameroil, which showed any uncharged droplets, and these were of all sizes. They formed about 25 percent of the drops observed.

It is quite clear that the phenomena involved here differ radically from those observed by Lenard and his group. It may be that the mechanism of charged drop production is different for drops of the two ranges of size. Or, perhaps, in the present work the charges were due to the presence of ionized particles in the organic substances used. Lenard's group sprayed water and estimated drop size from the mobilities of the ions found in the air carrying the spray particles. They could not possibly have observed the slow droplets studied here. What they studied were either initially created minute drops (of about 10^{-7} cm radius), or else larger droplets that had evaporated to the minute dimensions at which the charge on the droplet caused a balance between evaporation and condensation in the air blast used in the measurement. In the work on small drops a marked difference in mobility between positively and negatively charged drops was observed, and positively charged drops were found only in the case of salts dissolved in the water.[7]

It is clear that the relation between the charged droplets studied by Lenard and his group and those studied in this investigation can be determined only by a study of the mobilities and sign of the charges of drops of all sizes. To this end an ion mobility method of high resolving power, suitable to such an investigation, is being developed in this laboratory.

---

[7] On the contrary, Busse, reference 6.

Investigations of Turbulent Flow by Means of the Hot-Wire Anemometer

F. L. WATTENDORF AND A. M. KUETHE, *California Institute of Technology*
(Received March 24, 1934)

I. INTRODUCTION

TURBULENT flow is characterized by an irregular fluctuating motion superimposed on a mean flow. Reynolds,[1] in his analysis of turbulent flow, expressed the shearing stresses for a parallel mean flow in the x-direction

$$\tau_{xy} = -\rho\overline{u'v'}; \qquad \tau_{xz} = -\rho\overline{u'w'}, \tag{1}$$

where u', v' and w' are the fluctuations in the velocity in the direction and perpendicular to the direction of the mean flow, respectively, ρ is the fluid density and the bar indicates that the mean value of the product over the time has been taken. It is seen, then, that the turbulent flow of a fluid at a point is characterized by the magnitude of the components of velocity fluctuation together with the correlation between them, and experimental evidence concerning these quantities is of great importance for the development of a theory of turbulent flow.

The present work gives measurements of a root-mean-square value of the fluctuation in the direction of the main flow, i.e., $(\overline{u'^2})^{1/2}$ in various types of turbulent flow. The method used was that of the compensated hot wire anemometer, the investigations were made for the following cases:

1. Fully developed parallel flow.
2. Boundary layer along a flat smooth wall.
3. Fully developed curved flow.
4. Working section of 10′ wind tunnel with and without artificial turbulence (in correlation with sphere drag tests and maximum lift measurements).
5. Turbulence in the free atmosphere with airplane and blimp.

The compensated hot-wire circuit used in the present work is based in principle on the circuit developed by Dryden and Kuethe[2,3] at the Bureau of Standards. The reader is referred to references 2 and 3 for details of the analysis, since only the results will be given here.

II. DISCUSSION OF THEORY OF LAG OF HOT WIRE AND COMPENSATION

King's[4] equation for the heat loss from an electrically heated wire in a steady stream of fluid is

$$i^2R = (K + Cu^{1/2})(T - T_0) \tag{2}$$

where i = current flowing through the wire, R = resistance of the wire, K = proportionality factor allowing for free convection, C = proportionality factor allowing for forced convection, T = temperature of the wire, T_0 = temperature of moving fluid. If now the heated wire is placed in a flow in which the speed fluctuates within small limits, it is found that the instantaneous temperature of the wire is a function both of the amplitude and the frequency of the fluctuations. Within narrow limits (about 15 percent of the mean velocity) at a given frequency the amplitude of the temperature fluctuation is very nearly proportional to that of the speed fluctuation. If the amplitude remains constant and the frequency varies, as is shown in reference 2, the resistance fluctuation is cut down in the ratio

$$\left[\frac{1}{(1+M^2\omega^2)^{1/2}}\right]^{j\tan^{-1}M\omega}, \tag{3}$$

where M is the time constant of the wire and is given by

$$M = 4.2ms(\overline{T} - T_0)/i^2R_0. \tag{4}$$

[1] O. Reynolds, *An Experimental Investigation of the Circumstances which Determine Whether the Motion of Water shall be Direct or Sinuous and of the Law of Resistance in Parallel Channels*, Phil. Trans. Roy. Soc. **174**, 935 (1883).

[2] H. L. Dryden and A. M. Kuethe, *The Measurement of Wind Speed Fluctuations by Means of the Hot-Wire Anemometer*, N. A. C. A. Technical Report 320 (1929).

[3] H. L. Dryden and A. M. Kuethe, *Effects of Turbulence in Wind Tunnel Measurements*, N. A. C. A. Technical Report 342, (1930).

[4] L. V. King, Phil. Trans. Roy. Soc. (London) **A214**, 373 (1914).

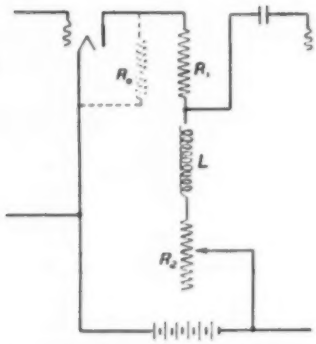

FIG. 1. Schematic diagram of compensation circuit.

In the above expressions $\omega = 2\pi$ times the frequency, m = the mass of the wire, $\overline{T}$ = mean temperature of the wire, s = the specific heat of the material of the wire, R_0 = resistance of the unheated wire. The phase lag expressed by the exponential term is important only when the actual shape of the fluctuations is being investigated.

The steady potential drop across the hot-wire terminals is balanced out by causing the wire to form one arm of a balanced Wheatstone bridge circuit. Then the fluctuations in voltage are impressed across the input of a vacuum tube amplifier. The root mean square of the current fluctuations in the output of the amplifier may be measured or the output may be used to actuate an oscillograph element. However, because of the above-mentioned lag of the hot-wire, the results would not be a true measure of the velocity fluctuations except for very low frequencies.

In order to counteract this lag, an electrical filter circuit of the type shown in Fig. 1 was included in the plate circuit of one of the amplifier stages. It consists of an inductance, a variable and a fixed resistance in series replacing the plate resistor. The drop in voltage across R_2 and L is passed on to the next stage. A complete discussion of this circuit is given in reference 2. It will only be noted here that a measure of the theoretical effectiveness of the compensation is given by the term

$$\omega L/(R_0+R_1+R_2) \tag{5}$$

and that the attenuation factor is approximately

$$R_2/(R_0+R_1+R_2). \tag{6}$$

It is seen that increasing the effectiveness of the compensation involves an increase in attenuation as well, and it becomes necessary then to adjust these two factors so that the performance of the entire arrangement will be as effective as possible without too much loss of amplification.

In 1930 Ziegler[5] reported on an equivalent circuit which had been used with success at Delft. The compensation was obtained by the use of a condenser, a parallel and a series resistance. The arrangement was in the input circuit, the drop across the series resistance being passed on to the amplifier. Mock and Dryden[6] pointed out that if the compensation is to be placed between two of the amplifier stages the performance of the inductance circuit is superior to that of Ziegler's arrangement.

The fluctuations in resistance of a single hot-wire actually represent, to a first order, only u', i.e., the velocity fluctuations in the direction of the main flow. This will be appreciated from the following analysis. Neglecting the lag of the wire, the instantaneous resistance corresponds to the velocity

$$q = [(\bar{u}+u')^2+v'^2+gw'^2]^{1/2},$$

where g is a factor, considerably less than unity, to allow for the fact that w' fluctuations are parallel to the wire. Since the steady voltage drop across the wire is balanced out, we pass on to the amplifier an instantaneous voltage corresponding to the velocity $a = q-\bar{q}$. The quantity measured by the mean square meter in the output corresponds to $\overline{a^2}$ and

$$\overline{a^2} = \overline{q^2}+\bar{q}^2-2\overline{q\bar{q}} = \overline{q^2}-\bar{q}^2,$$

since, by the rules for taking mean values $\overline{q\bar{q}} = \bar{q}^2$. Now, expanding $\bar{q}$ by means of the binomial theorem,

$$\bar{q} = \bar{u}\left[1+\tfrac{1}{2}\left(\frac{2u'}{\bar{u}}+\frac{u'^2}{\bar{u}^2}+\frac{v'^2}{\bar{u}^2}+g\frac{w'^2}{\bar{u}^2}\right)-\tfrac{1}{8}\cdot\frac{4u'^2}{\bar{u}^2}+\cdots\right]$$

$$= \bar{u}+\tfrac{1}{2}\left(\frac{\overline{v'^2}+g\overline{w'^2}}{\bar{u}}\right).$$

Squaring this quantity and subtracting from

[5] M. Ziegler, *The Application of the Hot-Wire Anemometer for the Investigation of the Turbulence of an Air-stream*, Proc. K. Akad. v. Wetenschappen Amsterdam 33.7 (1930).

[6] W. C. Mock and H. L. Dryden, *Improved Apparatus for the Measurement of Wind Speed Fluctuations*, N. A. C. A. Technical Report 448 (1932).

$\overline{q^2}$ we get

$$\overline{a^2} = \overline{u'^2}, \quad \text{approximately.} \qquad (7)$$

Obviously, if the velocity fluctuations are a considerable percentage of the mean velocity at the point, more terms must be taken in the above expansion and we then measure an appreciable part of the v' fluctuations.

III. Apparatus

The hot-wire used at the Guggenheim Aeronautics Laboratory, California Institute of Technology (abbreviated GALCIT) was of platinum 0.0147 millimeter in diameter and about three millimeters long. The diameter was measured by means of a travelling microscope and is probably correct to ± 0.0003 millimeter. The wire is welded across the terminals in the manner described in reference 3. The mounting is 3/32" drawn copper tube, bent at right angles one inch from the end nearest the hot-wire. An insulated wire running through the tube forms one terminal while a prong is fastened to the copper tube itself for the other terminal. Fig. 2 shows one of the hot-wires mounted in a micrometer screw for making traverses across a channel or through a boundary layer.

Fig. 3 is a wiring diagram of the circuit used. The amplifier and part of the input circuit were built up at this laboratory, and the whole was adapted by the authors to the measurement of turbulent fluctuations.

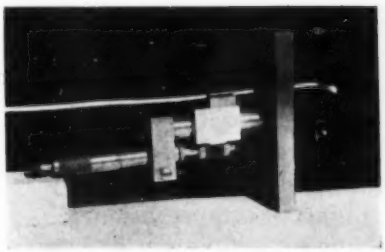

Fig. 2. Hot wire mounted on a micrometer traversing mechanism.

The hot-wire in series with a one-ohm resistance and a milliammeter forms one arm of a Wheatstone bridge. The bridge is adjusted so that only the fluctuations in voltage across it are passed on to the input transformer of the amplifier. The wire is operated at a constant current measured by means of the potentiometer arrangement across the one-ohm resistance in series with the hot-wire. By means of this arrangement the current can be adjusted to ± 0.4 milliampere.

The fluctuations are first amplified through two resistance-capacity coupled stages and then are fed into a three stage push-pull, transformer-coupled amplifier constructed by the General Radio Corporation. This unit is a.c. operated, the three stages using UY227, UX226 and UX250 tubes, respectively. The alternating current introduced a small hum in the amplifier but this was, at all times, small enough so that

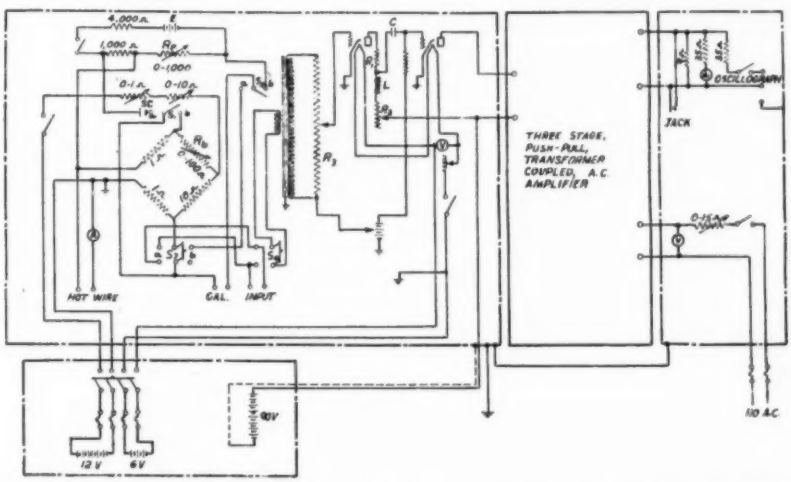

Fig. 3. Wiring diagram of the GALCIT hot-wire apparatus. Since the a.c. amplifier is of conventional type, the wiring diagram is not included. SC is a standard cell by means of which the voltage of E is determined. $R_1 = 10{,}000$ ohms, $L = 2.45$ henrys, $R_2 = 400$ ohms (about), $C = 2$ microfarads, A_1 is a Weston thermogalvanometer reading current squared.

its subtraction did not sensibly impair the accuracy of the results. With the compensation circuit removed the five stages gave an amplification which was constant with frequency to within five percent from 50 to 8000 cycles. This was considered a satisfactory framework in which to install compensation.

The compensation circuit was designed with recourse to expressions (5) and (6), respectively. The constants of the circuit used were $L=2.45$ henries, $R_0=10{,}000$ ohms, $R_1=10{,}000$ ohms, $R_2=400$ ohms (approximately). With these values (5) gives an error factor of 1.20×10^{-4} from which we deduce that the error in compensation is one percent at a frequency of 185 c.p.s., and seven percent at 500 c.p.s. The attenuation factor, calculated from (6) is 0.0196. For the scale at which measurements were made oscillograms showed that frequencies above 500 c.p.s. were of secondary magnitude.

Fig. 4 shows curves for the amplifier response with compensation, the lag of the hot-wire for $M=0.0036$ and the result of the multiplication of these curves. The latter represents the overall response of the hot-wire, compensation and amplifier. Actually, the error factor mentioned above was only five percent at 500 c.p.s. and about ten percent at 800 c.p.s.

The calibration procedure, giving the amplifier curve in Fig. 4, was as follows: The hot-wire was replaced by an equivalent constant resistance through which an alternating current of known frequency and amplitude, generated by a vacuum tube oscillator, was passed. The bridge was then connected across the input of the amplifier and the output was measured on a mean square

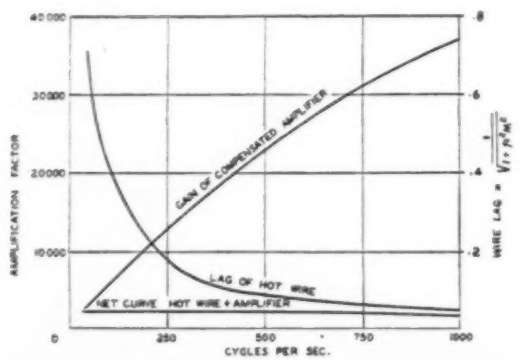

FIG. 4. Curves of hot-wire lag, gain of compensated amplifier, and gain of hot-wire plus compensated amplifier.

galvanometer. This was carried out for various frequencies from 50 to 1000 c.p.s., and for various values of the compensation resistance R_2 with and without inductance. By placing the same resistance across the terminals marked input and closing switch S_4 the procedure was repeated. Then the ratio of these results to those obtained with the resistance in the bridge circuit (after applying a correction term resulting from the fact that the resistance was actually in parallel with the bridge circuit) gives the bridge factor, i.e., the factor by which the bridge cuts down the response because of the drop through the hot-wire, the one-ohm resistances and the milliammeter. It was found that the bridge factor did not vary by more than five percent in the entire range of frequencies, and from this it was concluded that the impedance of the input transformer was so large that it could be disregarded insofar as it might alter results. The value of the inductance used is really an effective inductance calculated from the slope of the amplification curve of the compensated amplifier and the amplification for $L=0$ and $R_2=1$ ohm. The attenuator designated by R_2 has fifteen taps by means of which the amplification can be varied from full to practically zero amplification. This was also calibrated by means of the oscillator.

The procedure of making turbulence measurements will be described briefly. The positions of the various switches can be determined from Fig. 3. The measurements were generally made at various positions along a lateral traverse of a channel, or through a boundary layer, and consisted of about ten measurements at as many stations. Before and after each traverse, it was necessary to measure the resistance of the wire at room temperature and to take a calibration of resistance of the wire against mean wind speed at the heating current used for the measurements. For the former, a very small current was passed through the bridge and by adjusting R_B, a balance was obtained. For the latter, the hot-wire was placed at a position where the mean speed was known as a function of the static pressure at the wall of the channel. Maintaining a constant heating current, readings of the resistance of the hot-wire were taken at a series of wind speeds covering the range encountered

in the traverse. Then, plotting $i^2RR_0\alpha/(R-R_0)$ *versus* $u^{1/2}$ results in a straight line. That this is true is easily seen from a consideration of Eq. (8) below, which is Eq. (2) in a slightly different form. As is shown below, the slope of this line is used in the calculation of the velocity fluctuations. There was generally a slight divergence between the two calibration curves but the slopes were usually within 5 percent of each other.

At each position of the traverse readings were taken of the mean resistance of the wire, the attenuator tap used and the root-mean-square value of the output as read by a thermal ammeter. Also at each position the time constant of the wire was calculated according to (4), and the compensation resistance adjusted to its correct value so that the amplitudes of the fluctuations would be reproduced in the correct relation with each other.

The reading of the thermal galvanometer cannot be interpreted directly in terms of velocity fluctuations since any voltage fluctuation across the wire is accompanied by a change in the heating current. Fig. 5 is a schematic diagram of the circuit considered. Since $T-T_0=(R-R_0)/R_0\alpha$ Eq. (2) can be expressed in the form

$$i^2RR_0\alpha/(R-R_0)=K+Cu^{\frac{1}{2}}. \tag{8}$$

Differentiating this expression with respect to i, R and u gives

$$\frac{2iRR_0\alpha}{R-R_0}di-\frac{i^2R_0^2\alpha}{(R-R_0)^2}dR=\frac{Cdu}{2u^{\frac{1}{2}}}$$

and this, along with the relations

$$E=i_0r_1+i(R+r_2),$$
$$i_0=i+i_3;\quad i_3=i(R+r_2)/r_3,$$
$$E_b(di/i^2)=-(r_1/r_3+1)dR,$$
$$dE=idR+Rdi,$$

where $r_2=r_4+r_5$, gives the result

$$du/u=-(2/Cu^{\frac{1}{2}})[F+GB]dE/(1-RB),$$

where $F=iR_0^2\alpha/(R-R_0)^2$,

$G=2iRR_0\alpha/(R-R_0)$,

$B=(E+ir_3)/E_b(r_3+r_2+R)$.

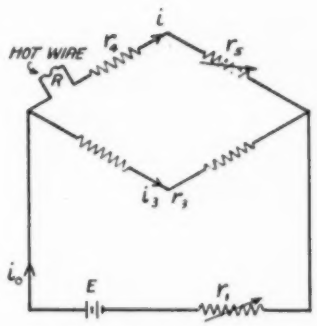

FIG. 5. The bridge circuit.

In the above formula du is really $[\overline{u'^2}]^{\frac{1}{2}}$ since $dE=(\overline{\Delta E^2})^{\frac{1}{2}}$. dE is found by dividing the output voltage by the overall amplification factor which includes the bridge factor previously discussed. The fact that the heating circuit was disconnected for the calibration of the amplifier with the vacuum tube oscillator actually causes a very slight error.

IV. Distribution of Velocity Fluctuations Through a Channel

One of the fundamental problems in the study of turbulent flow is that of the mechanism of the transport of momentum in parallel or nearly parallel flow. Several theories have been advanced for the solution of this problem, but for experimental checking it would be necessary to have measurements of the actual components of velocity fluctuations, u' and v'. The present measurements give only the root-mean-square values of u', the component parallel to the mean flow. Measurement of the perpendicular component v' and the correlation between u' and v' are in progress at the California Institute of Technology.

Most of these measurements were made in a channel previously used by F. L. Wattendorf[7] for the investigation of curved flow. The channel, shown in Fig. 6, has a breadth of 5 centimeters and a depth of 90 centimeters so that the ratio of depth to breadth is 18 : 1. The ratio was chosen large in order to avoid, as much as possible, the disturbing influence of the top and bottom, or, in other words, so that the mean flow in the section at one-half the channel depth would be approximately two-dimensional.

[7] To be published at an early date.

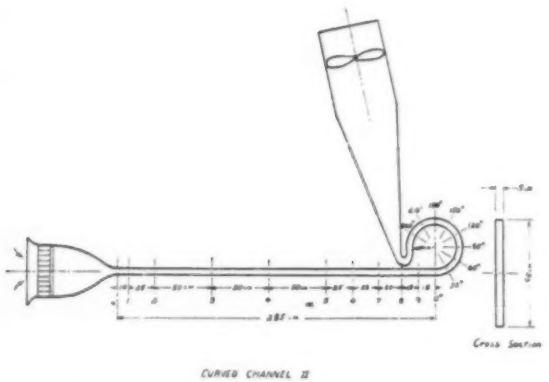

FIG. 6. Diagram of curved channel showing the various measurement stations.

The channel consisted of a bell-shaped entrance, with honeycomb, leading into a straight section with parallel walls 285 centimeters long. The purpose of the straight section was to build up the flow into a fully developed turbulent state. This length is 57 times the channel breadth b, and previous investigations showed that the flow was in a fully developed state at the measuring section. The straight section, in turn, leads into a curved section, with the walls formed into concentric circular arcs, of inner radius 20 centimeters and outer radius 25 centimeters. The curvature extends through about 300° of arc, in order to obtain a fully developed curved flow. Fastened to the end of the curved section is a transition section leading to the propeller and motor unit.

The measurement stations are also shown on the diagram. The hot-wire was projected through a hole in the tunnel wall, and its micrometer mounting (see Fig. 2) by means of which traverses were made, was securely fastened to the outside. A static orifice at each station measured the wall pressure at that point.

Two different experimental techniques were used at section 9 which represents fully developed straight flow. The values of $\overline{u'^2}/u^2_{\max}$ obtained from both methods are given in Fig. 7 and it is seen that they check rather well with each other. The first method consisted of operating the hot-wire under conditions such that a constant value of M, the time constant of the wire, would be preserved at all times. This meant that at every position during a traverse, the current through the wire had to be

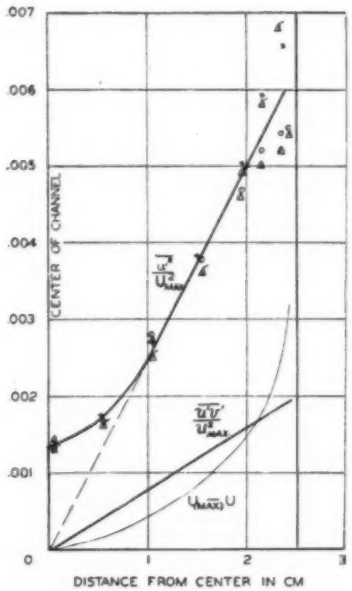

FIG. 7. $\overline{u'^2}/u^2_{\max}$ and $-\overline{u'v'}/u^2_{\max}$ *versus* distance from the center for fully developed straight flow.

adjusted to a value which would keep the ratio $i^2/(R-R_0)$ a constant. The second method involved the use of a constant heating current (usually 0.16 ampere) and calculating M and R_2 for each point. The latter method was adopted as the standard procedure because of its greater ease of application.

The distribution of $\overline{u'^2}/u^2_{\max}$ for the fully developed straight flow is given in Fig. 7, and the significant thing is that a straight line can be passed approximately through all points except those near the wall and near the channel center. It is well known that for a fully developed parallel flow the friction varies linearly from a value of $(b/2)(dp/dx)$ at the walls, where dp/dx is the pressure drop in the channel and b is the channel breadth, to zero at the center. The distribution of $\tau/\rho u^2_{\max}$ which, according to (1), is equal to $-\rho\overline{u'v'}/u^2_{\max}$ is shown also in Fig. 7. Comparison of the two linear distributions shows that

$$-\overline{u'v'}/\overline{u'^2}=0.3$$

approximately holds in the linear region.[8]

[8] Since the completion of this work an investigation by H. Reichardt (Zeits. f. Angew. Math. u. Mech. (13), 3, 177–180 (1933)) has been reported, in which measurements of $(\overline{u'^2})^{\frac{1}{2}}/u$ are made in rectilinear fully developed flow at a low scale. Measurements at a low mean velocity with an uncompensated hot-wire are given. Plotting of $-\overline{u'v'}/\overline{u'^2}$

The above results indicate a constant correlation between $\overline{u'v'}$ and $\overline{u'^2}$. In the theory of turbulence the quantity $-\overline{u'v'}/(\overline{u'^2})^{\frac{1}{2}}(\overline{v'^2})^{\frac{1}{2}}$ is used as a "correlation factor" and we need to know this quantity, along with the magnitude of the fluctuations, in order to fully characterize turbulent flow. If now we assume similarity of the turbulence mechanism, as proposed by von Kármán,[9] which implies that the ratio of $(\overline{u'^2})^{\frac{1}{2}}/(\overline{v'^2})^{\frac{1}{2}}$ is constant, then $\overline{u'v'}/\overline{u'^2}$ is proportional to $\overline{u'v'}/(\overline{u'^2})^{\frac{1}{2}}(\overline{v'^2})^{\frac{1}{2}}$, and our results indicate therefore a constant correlation factor for straight flow. It may be mentioned that Prandtl's[10] mixing length theory contains the assumption that $|u'|$ and $|v'|$ are both proportional to $l(du/dy)$, where l represents the so-called mixing length, so that this theory also implies constant correlation. A final proof of the assumption of constant correlation can only be found by direct measurement of $(\overline{v'^2})^{\frac{1}{2}}$ for which measurements are now being prepared in this laboratory. It may be mentioned that measurements by Fage,[11] carried out by means of an ingenious optical method, show that for turbulent flow in a square channel, the maxima of u', v', w' are nearly equal in the region excluding the wall neighborhood. Also observations by Taylor[12] of atmospheric turbulence, which represents a turbulent flow of large magnitude and low frequency, show that except near the ground u' and v' are nearly equal.

For the purpose of investigating scale effect on the magnitude of the fluctuations, measurements were made at the channel center at section 9 for various mean speeds from 7 to 25 meters per second. Previous measurements of the mean velocity profiles showed the effect of Reynolds number on the velocity distribution to be small. The measurements of $(\overline{u'^2})^{\frac{1}{2}}/u_{\max}$, however, showed a definite decrease with increasing velocity, and the question is, on what physical parameters is the scale effect based. Since the shearing stress is proportional to the product of the fluctuation components it would seem reasonable to assume a dependence of $\overline{u'^2}$ on the shearing stress at the wall τ_0. Accordingly, the curve of $(\overline{u'^2})^{\frac{1}{2}}/u_{\max}$ against R.N. was compared with that of $K(dp/dxb/\rho)^{\frac{1}{2}}/u_{\max}=K(2\tau_0/\rho)^{\frac{1}{2}}/u_{\max}$ *versus* R.N. where K was arbitrarily chosen to bring the curves at the same level for purposes of comparison. Fig. 8 shows the result, and it is seen that the curves are similar, although the range of scale covered was not large enough to make any definite conclusions.

However, it seemed possible that the magnitude of the fluctuations in the channel center might also be dependent on entrance conditions. Accordingly, screens of various sizes were introduced just ahead of section 1, and the traverse at section 9 repeated. It was found that the distribution of $(\overline{u'^2})^{\frac{1}{2}}$ at section 9 was unaffected by the presence of the screens. It is well known that the mean velocity distribution in fully developed turbulent flow is not affected by disturbances at the entrance of the channel. It follows, then, that if the fluctuation level were raised by the above procedure, it must be accompanied by a weakened correlation in order that the shearing stress remain unchanged. The results indicate, then, that in fully developed turbulent flow, the fluctuations in velocity have reached a statistical equilibrium and the correlation factor is unaffected by fluctuations introduced at the entrance.

Traverses were also made at stations 2 and 3 in the entrance section in order to study the

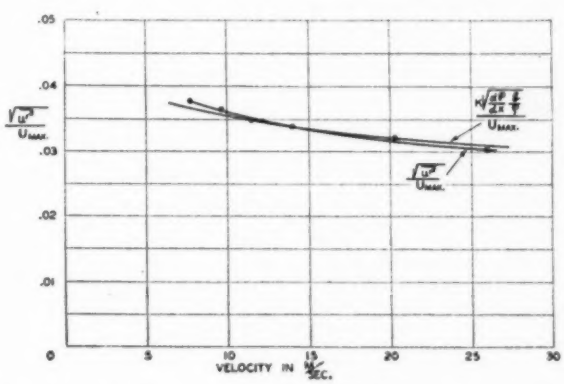

FIG. 8. The effect of scale on $(\overline{u'^2})^{\frac{1}{2}}/u_{\max}$ at the center of section 9.

over the section results in an approximately constant value of 0.24 over a large part of the region excluding the neighborhood of the walls and channel center.

[9] Th. von Kármán, *Mechanical Similitude and Turbulence*, Nachr. Ges. Wiss., Goettingen, 58–76 (1930).

[10] L. Prandtl, *Bericht über Untersuchungen zur Ausgebildeten Turbulenz*, Zeits. f. Angew. Math. u. Mech. **5**, 136 (1925).

[11] A. Fage, *Study of Turbulent Flow by Means of the Ultra-Microscope*. Proc. Roy. Soc. **A135**, 828, 656 (1932).

[12] G. I. Taylor, Turbulence, Roy. Met. Soc. J. **53**, 201–212 (1927).

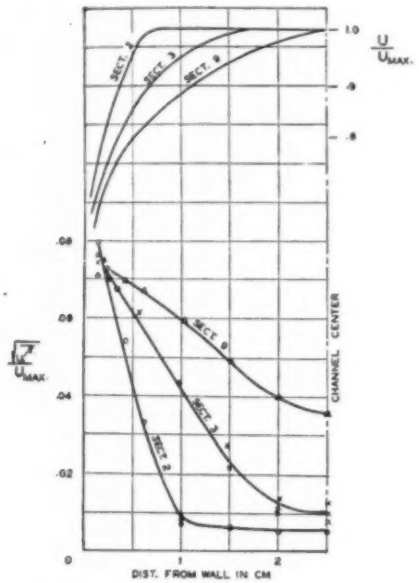

FIG. 9. $(\overline{u'^2})^{\frac{1}{2}}/u_{\max}$ and $u/u_{\max}$ for two stations near the entrance of the channel. For comparison the results for fully developed straight flow are reproduced.

development from boundary layer flow to fully developed turbulence. The results are shown in Fig. 9, along with the mean velocity profiles. Section 2 indicates a distinct boundary layer at each wall separated by a region of potential flow in the center. The magnitude of the fluctuations decreases rapidly through the boundary layer to a constant low value of about 0.5 percent in the region between the boundary layers. At section 3 the velocity profile still indicates two distinct boundary layers, separated by a rather narrow gap, but the rise in turbulence level at the center indicates that there is already considerable turbulent interchange between the boundary layers. It is significant that the magnitude of the fluctuations near the wall is of the same order for all sections.

V. Measurements in the Curved Channel

Traverses of $(\overline{u'^2})^{\frac{1}{2}}$ as well as mean velocity were taken at various stations in the curved portion of the channel. The results are shown in Fig. 10. For convenience the ordinates are displaced vertically by the amounts indicated.

The fluctuation profiles throughout the transition region from fully developed straight to fully developed curved flow show two predominating tendencies. The first is a general flattening of the profile in the central region of the channel. This is closely analogous to the corresponding velocity profiles, which show that the mean flow in the corresponding region approaches the potential distribution $ur = \text{constant}$, where r is the radius at the considered point. The second tendency is that the gradient of $(\overline{u'^2})^{\frac{1}{2}}$ is steeper at the outer wall and flatter at the inner wall than for straight flow. This is probably associated with the different states of stability at the two walls. At the outer wall the centripetal pressure gradient is directed away from the wall, giving rise to instability of the turbulent exchange, while at the inner wall the pressure gradient is directed towards the wall, which produces a stabilizing effect. It is interesting to note that both of the above tendencies fluctuate about the final distribution at the 210° section. It is to be expected that $(\overline{v'^2})^{\frac{1}{2}}$ should be rather strongly affected by curvature, and measurements of $(\overline{v'^2})^{\frac{1}{2}}$ are necessary for further treatment of the problem of curved flow.

VI. Investigations with Acoustic Analyzer

The work of Mock and Dryden[6] indicates that, in general, it would not be possible to express the fluctuations as the superposition of a number of components of different frequencies. In other words, while any single oscillograph record of the fluctuations could be represented by a Fourier series, it would not be possible to use this series to describe another record. An attempt to investigate this same problem was made at this Institute and gave negative results. An acoustic analyzer designed by Mr. L. P. Delsasso of the University of California at Los Angeles was kindly loaned to the authors. It is essentially a quadrant galvanometer with the mirror mounted on a trifilar suspension, the fundamental frequency of which could be varied from 50 to 500 c.p.s. by varying the tension of the wires. Since the analyzer is a voltage device it is necessary to connect it across a step-up transformer in the output of the amplifier. The hot-wire was placed in a fully developed turbulent flow and the fluctuations in voltage passed on to the amplifier, the output of which actuated the analyzer. While a slight response was detected at several points in the frequency range attain-

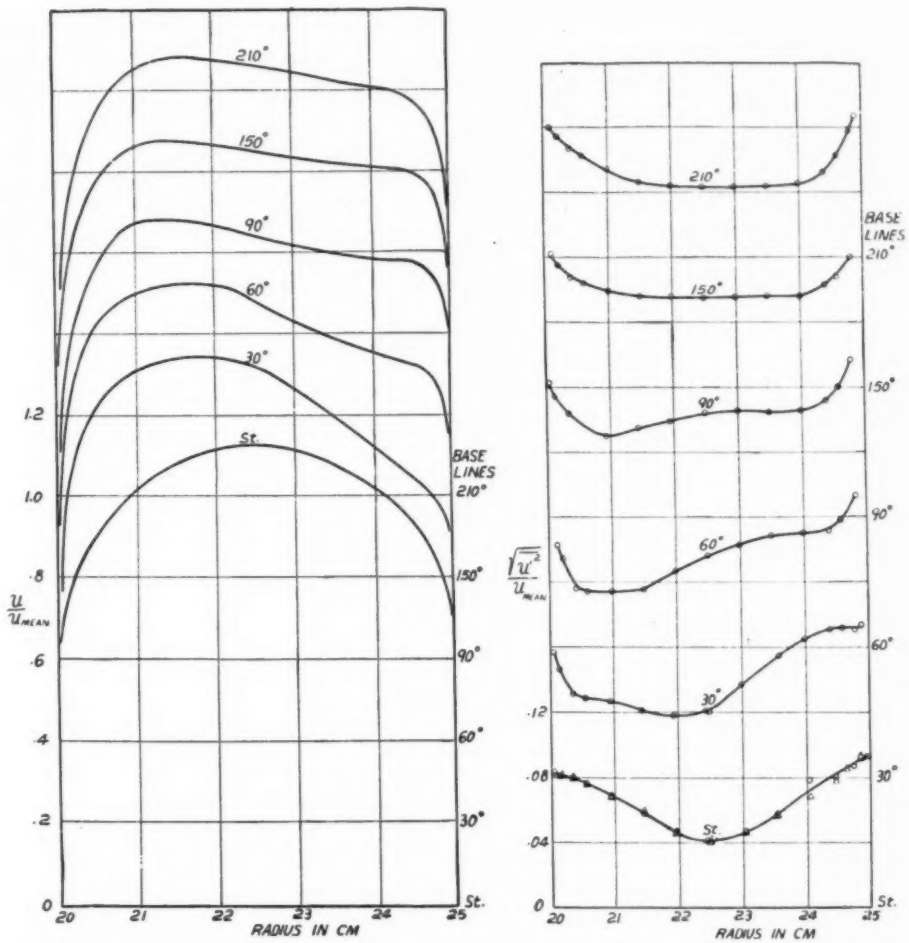

FIG. 10. u/u_{mean} and $(\overline{u'^2})^{\frac{1}{2}}/u_{\text{mean}}$ for various positions from fully developed straight to fully developed curved flow. For section 9 the abscissa denotes distance from a line parallel to the straight portion passing through the center of curvature for the curved portion. For convenience the ordinates for the various profiles are displaced vertically by the amounts indicated. $u_{\text{mean}} = 12.4$ meters per second.

able, the amplitude of the mirror oscillation did not reach a steady value, indicating that the phase of the disturbances was continually changing. Fig. 11 is an oscillograph record of fully developed turbulent flow and illustrates the apparently random character of the fluctuations.

VII. Wind Tunnel Measurements

Experimental determination of the magnitude of turbulent fluctuations in wind tunnels is highly important because of the fact that certain types of aerodynamic measurements are greatly influenced by turbulence. For instance Dryden and Kuethe[3] and later Dryden[13] showed that in fact a marked correlation exists between the critical Reynolds number of a sphere and the percentage magnitude of the velocity fluctuations present in the air stream. The critical Reynolds number was defined as that Reynolds number at which the sphere drag coefficient was 0.3. This point falls in the vicinity of the center of the more or less sudden break which occurs in the curve of drag coefficient *versus* Reynolds number.

Recent experiments in the GALCIT 10′ tunnel have shown that also the maximum value of the lift coefficient of airfoils depends largely on the degree of turbulence in the air stream. Drs. C. B. Millikan and A. L. Klein[14] made an extensive

[13] H. L. Dryden, *Reduction of Turbulence in Wind Tunnels*, N. A. C. A. Technical Report 392 (1931).

[14] C. B. Millikan and A. L. Klein, *Effects of Turbulence*, Aircraft Engineering, August (1933).

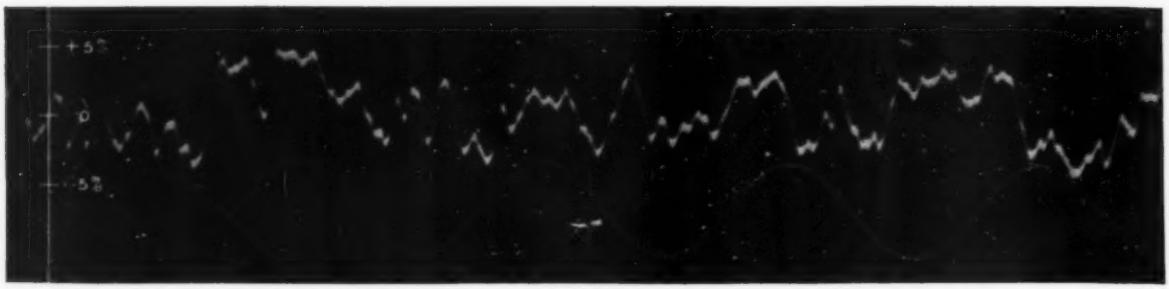

FIG. 11. Oscillogram of rectilinear fully developed straight flow taken at the center of the channel. A fifty c.p.s. timing wave is shown along with an approximate magnitude scale. $u_{\text{mean}} = 12.4$ meters per second.

series of measurements investigating the effect of artificially created turbulence on the stalling point, or $C_{L(\max)}$ of airfoils. Different degrees of turbulence were produced by mounting a grid composed of 1/8 inch diameter rods, spaced 3/4 inch apart, at various distances upstream from the model.

In order to correlate the values of $C_{L(\max)}$ with the critical Reynolds number of spheres, and with the percentage of velocity fluctuations, the airfoil model was first replaced by a sphere, and the critical drag curves obtained. Then the sphere was replaced by the hot-wire, and turbulence measurements were carried out. Fig. 12 shows the grid with the sphere in place. Fig. 13 shows the curves of sphere drag coefficient C_D *versus* R.N. for various distances of the grid upstream from the sphere. R_{crit}, as mentioned above, is the R.N. for which $C_D = 0.3$ in each case.

The results of the hot-wire measurements are shown in Fig. 14, where $(\overline{u'^2})^{\frac{1}{2}}/u$ is plotted as a function of stream velocity for the clear tunnel and two grid positions. In order to correlate the values of R_{crit} with the turbulence, the values of $(\overline{u'^2})^{\frac{1}{2}}/u$ were taken from the curve of Fig. 14, at the same value of tunnel speed at which R_{crit} occurred for the corresponding sphere drag test at the same grid position. The correlation between R_{crit} and the fluctuations, obtained in this way, is shown in Fig. 15. In this figure are included the data of Dryden taken at the Bureau of Standards. It is remarkable that the values fit well on one curve, especially since Dryden used several different tunnels, and his apparatus was different in detail.

Fig. 16 shows the correlation between $C_{L(\max)}$ and the velocity fluctuation $(\overline{u'^2})^{\frac{1}{2}}/u$. The curve was obtained in the following way: First curves of $C_{L(\max)}$ *versus* R_{crit} were plotted for several Reynolds numbers of the airfoil. Then the values of $(\overline{u'^2})^{\frac{1}{2}}/u$ for the different values of R_{crit} were taken from the curve in Fig. 15, and the curves of $C_{L(\max)}$ *versus* $(\overline{u'^2})^{\frac{1}{2}}/u$ for several R.N.'s of the airfoil were plotted. In Fig. 15 the three lower

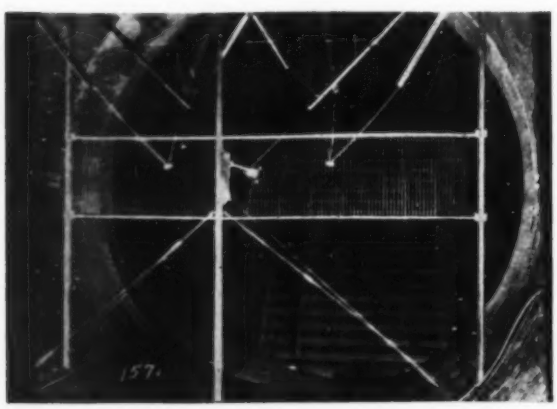

FIG. 12. The grid in position ahead of a sphere.

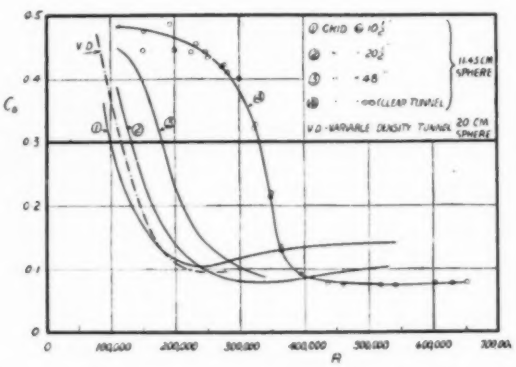

FIG. 13. Sphere drag coefficient drag/$(\rho/2u^2 \cdot \pi/4D^2)$ *versus* Reynolds number for sphere at various distances behind the grid. Reproduced from paper by Millikan and Klein, reference 14.

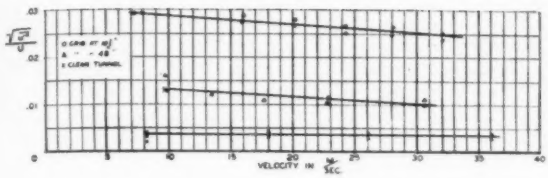

FIG. 14. $(\overline{u'^2})^{\frac{1}{2}}/u$ at various positions behind the grid.

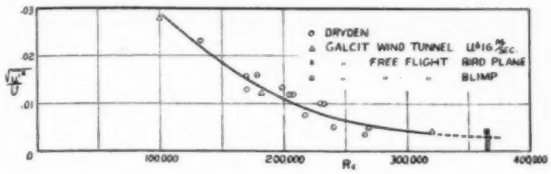

FIG. 15. The critical Reynolds number (R_c) of a sphere as a function of $(\overline{u'^2})^{\frac{1}{2}}/u$.

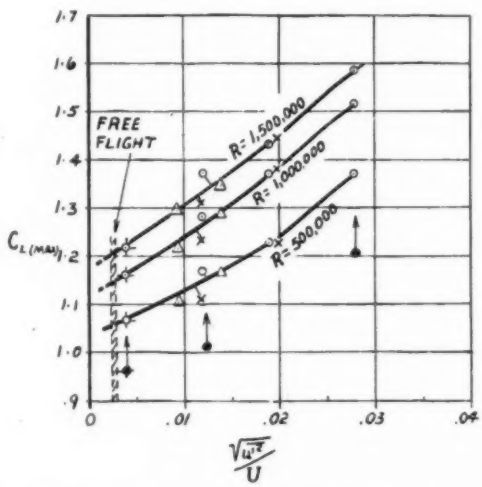

FIG. 16. The maximum lift coefficient, ($C_{L(\max)}$ of an airfoil as a function of $(\overline{u'^2})^{\frac{1}{2}}/u$.

black dots indicate only the level of $(\overline{u'^2})^{\frac{1}{2}}/u$ actually measured in the present investigation.

VIII. Free Flight Measurements

The discovery of the correlation between the maximum lift and turbulence indicated the necessity of a study of the degree of turbulence encountered by an airfoil in flight. Accordingly, Dr. Millikan made an extensive series of free air sphere drag measurements in which the sphere was mounted on one of the struts of a Bird biplane. One might expect that due to turbulence in the free air, the critical Reynolds number of the sphere would be lower than in the wind tunnel. However it was higher than that found in the GALCIT wind tunnel and it was apparently almost independent of air conditions and altitude. In view of this fact it seemed to be interesting to obtain data on the fluctuation of the velocity relative to the plane during flight, and to obtain oscillograms of atmospheric turbulence. Therefore, a hot-wire apparatus was built into a portable form and installed in the Bird biplane used for the sphere tests. The sphere and hot-wire were mounted at corresponding positions with respect to the fuselage.

Due to limitations in space there was little opportunity to shield properly the apparatus against vibration and electrostatic interference from the ignition system, and the hum level arising from these factors was so high that it was not possible to make accurate velocity fluctuation measurements. Oscillograms were taken on a special oscillograph designed by Mr. L. P. Delsasso and loaned to the authors. These oscillograms showed a large percentage of periodic fluctuations which almost certainly had their origin in either mechanical or electrical interference.

Some estimates were made of the root-mean-square value of the fluctuations at various speeds, both with power on and in a glide with the propeller turning over slowly. Then, for the purpose of obtaining a rough approximation to the amplifier hum, readings were taken under the same conditions with the wire unheated. Subtracting the hum from the mean square value of the output gave a turbulence level approximately the same as that in the air stream of the GALCIT wind tunnel. However, since it is likely that vibrational effects increase with wire sensitivity, this value probably represents an upper limit of the turbulence. The value found is shown in Fig. 15 plotted against the critical Reynolds number of the sphere.

IX. Blimp Measurements

More satisfactory measurements of atmospheric turbulence were made by installing the hot-wire apparatus in the Goodyear blimp Volunteer. The apparatus was well shielded from vibrational and electrostatic interference.

The mounting for the wire on the blimp consisted of a 1 inch steel tube 12 feet long lashed to the bottom of the control car so that the hot-wire, mounted on the end of the tube, was situated about 8 feet in front of the control car and about 10 feet below the bag. To simplify measurement procedure in the air, the hot-wire was calibrated immediately before the flight in an air stream produced by a variable speed vacuum cleaner.

Unfortunately, the blimp's stay in Los Angeles was very short and it was possible to make only one flight, on a day which was quite gusty. During the flight it was noticed that the main gusts had a period of about 5 to 30 seconds and were 3–4 m.p.h. in magnitude. Fluctuations of the balancing galvanometer of the Wheatstone bridge indicated, in addition, the presence of gusts of frequencies between 1 and 10 per second and about 1–2 m.p.h. in magnitude.

The fluctuations to which the amplifier system responded (from 50 to 1000 c.p.s.) were very irregular. The output meter registered practically zero a large part of the time, but during gusts made momentary excursions, the maxima of which were recorded. The magnitudes of these maxima are shown in Fig. 16 where they are plotted against the critical Reynolds number of the sphere as found in the previous investigation. The nature of the higher frequency fluctuations is shown in the oscillograph records of which Fig. 17 is a sample. For comparison an oscillogram of the turbulence in the GALCIT wind tunnel is shown in the same figure.

The measurements would seem to indicate that velocity fluctuations encountered by aircraft in flight are essentially of low frequency, and those of higher frequency, i.e., those which are significant for boundary layer stability, are of secondary magnitude.

Conclusions

The results obtained, both at this Institute and in other laboratories, by means of the hot-wire anemometer, indicate the feasibility of this method for a study of some of the fundamental laws governing turbulent flow. A complete study, including flow in various types of channels (convergent, divergent, etc.), of $(\overline{u'^2})^{\frac{1}{2}}$ and, especially $(\overline{v'^2})^{\frac{1}{2}}$, would add greatly to our knowledge of this branch of Fluid Mechanics.

The conclusions drawn, on the basis of the results given here, are:

1. That velocity fluctuations in rectilinear fully developed turbulent flow probably obey the laws of mechanical similitude as put forth by von Kármán.

2. That the shearing stress distribution determines the distribution of the root-mean-square value of the velocity fluctuations.

3. That the fluctuations are of a statistical nature and, in fully developed turbulent flow, the root-mean-square value is independent of channel entrance conditions.

4. That characteristic curves, such as sphere drag or $C_{L(\max)}$, can be correlated with $(\overline{u'^2})^{\frac{1}{2}}/u$.

5. That atmospheric turbulence apparently consists of large scale gusts, which themselves embody gusts of much smaller scale. The results given here, along with the results of Millikan and Klein, indicate that only the gusts of smaller scale affect boundary layer stability.

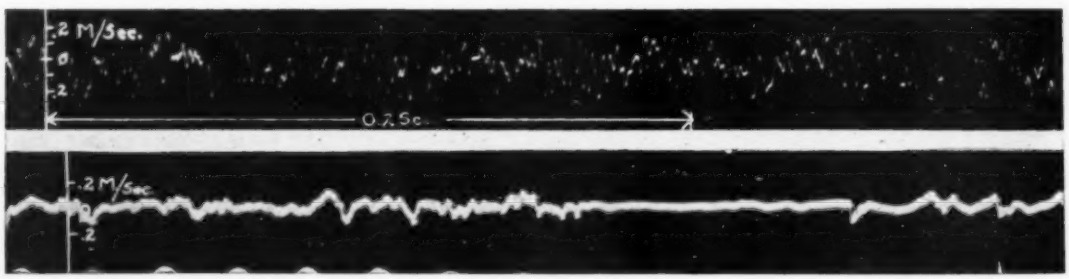

Fig. 17. Oscillograms of wind tunnel and atmospheric turbulence. The upper represents turbulence in the free stream of the GALCIT 10′ wind tunnel ($V=29$ meters per second) $(\overline{u'^2})^{\frac{1}{2}}/u=0.4$ percent approximate time and magnitude scales are shown. The lower record was taken during the blimp investigation ($V=19$ meters per second). The tops of a 50 c.p.s. timing wave can be seen at the lower edge.

Propagation of Elastic Waves in Ice. Part I

MAURICE EWING, A. P. CRARY AND A. M. THORNE, JR., *Lehigh University*

(Received February 23, 1934)

Measurements of the velocity of sound vibrations in ice have been made in some detail both by direct and resonance methods. The velocity of longitudinal waves was measured directly on large bodies of ice. Blasting caps were used to create elastic disturbances and the time of travel was recorded by an electric seismograph placed at suitable distances. A plot of time against distance gives a remarkably straight line showing a velocity of 3410 m/sec. Laboratory measurements were made on long thin rods of ice which were excited by an oscillator and resonance frequencies measured both for longitudinal and torsional vibrations. The velocities for these vibrations are found to be 3163 m/sec. and 1913 m/sec., respectively. A formula is derived by which the velocity of longitudinal waves in a thin infinite plate can be found from these velocities. This formula gives a value of 3400 m/sec. which checks with that obtained directly by less than one percent. Various other elastic constants for ice are also deduced from these measurements. The values of Young's modulus and Poisson's ratio for ice are found to be 9.17×10^{10} dynes/cm^2 and 0.365, respectively, in the range -5°C to -15°C.

INTRODUCTION

THE measurements made upon the elastic constants of ice up to about 1929 gave widely discordant results, principally because the early measurements were carried out by static methods which are ill suited to a substance whose elasticity is as imperfect as that of ice. The methods which have been applied may be listed for convenience in three classes: (a) Static methods, including all cases of stretching, bending, or twisting in which a steady stress is applied and the resulting strain measured; (b) Resonance vibration methods, in which the natural frequency of a characteristic mode of vibration of a small sample of ice is observed; (c) Direct velocity determination, in which the time for an impulsive elastic disturbance to travel a known distance is observed. In the present paper there are results obtained by the two latter methods. These results agree well with each other.

THE RESONANCE VIBRATION METHOD

1. Apparatus and method

The specimens of ice used were formed into rods usually a few centimeters in diameter and of the order of one meter in length. Both longitudinal and torsional vibrations were produced in these rods. The apparatus used is sketched in Fig. 1. For the longitudinal vibrations, a small iron disk of mass about 10 g was attached to each end of the bar. Short pieces of thin ebonite rod frozen into the ends of the bar afforded anchorage for the disks. To produce the vibration a telephone receiver with the diaphragm removed was placed near one of the disks and fed from the output of a General Radio Low Frequency Oscillator. A similar telephone receiver unit placed near the other disk served to detect longitudinal vibrations but was insensitive to vibrations of other types. The currents generated by this detecting system were fed through an amplifier into an a.c. voltmeter.

For torsional vibrations a small solenoid (mass about 15 g) was attached to each end of the rod to be tested, being anchored by a small piece of ebonite rod frozen into the ice. As is shown in Fig. 1 the axis of the solenoid was

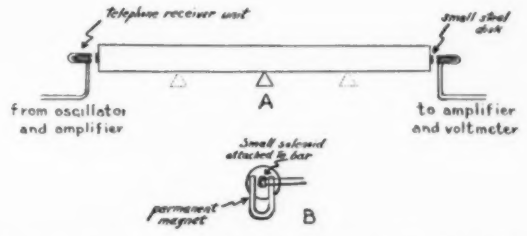

FIG. 1. A, side view of apparatus used to obtain longitudinal vibrations; B, end view of apparatus used to obtain torsional vibrations.

placed at right angles to the axis of the rod and a permanent magnet was placed to produce a magnetic field at right angles to both of these axes. Thus when alternating current of a suitable frequency was fed into the solenoid, torsional vibrations of the rod were produced. A similar arrangement of solenoid and magnet on the other end of the rod was connected through the amplifier to the a.c. voltmeter and served to detect torsional vibrations while remaining insensitive to vibrations of other types.

For both types of vibrations the voltmeter which served as detector of resonance gave very sharp indications of resonant frequencies. A telephone receiver was substituted for voltmeter at each resonance setting in order to decide whether the rod was resonating to the fundamental note of the oscillator or to an overtone of this note. A beat-frequency oscillator was found to be very useful for determining the approximate frequencies of resonance because of the ease with which its frequency could be continuously varied.

2. Results from the resonance vibration method

Measurements were made upon four rods of ice. Rods 1 and 2 were cut from a large block of artificial ice, in such a way that the "grain" of the ice—the direction in which the freezing had progressed—was perpendicular to the length of the rod. Rods 3 and 4 were formed by allowing water to freeze slowly and without stirring in vertical brass tubes. Since no other precautions were taken regarding the crystal orientation, the agreement of the results seems to indicate that this factor is of little importance in our work. The dimensions of the rods were as follows:

Rod	Length	Cross section
1	112 cm	5 cm×4 cm
2	99 cm	6 cm×5.5 cm
3	72.5 cm	diam. = 3.8 cm
4	117 cm	diam. = 3.8 cm

The results are summarized in Tables I and II. The wave-lengths listed are twice the length of the rod divided by the number of nodes. The rod frequencies, when they differ from the oscillator frequencies, are harmonics of the latter. The velocities are products of wave-length by frequency.

TABLE I. *Velocity of longitudinal vibrations in thin rods of ice.*

Rod	Wave-length cm	Oscillator frequency cycles/sec.	Rod frequency cycles/sec.	Velocity m/sec.	Residual m/sec.
1	224	1386	1386	3105	+58
1	224	693.1	1886.2	3105	+58
1	224	467.2	1401	3140	+23
1	224	354.5	1418.0	3176	−14
1	224	1387	1387	3107	+56
1	112	2884	2884	3230	−63
1	74.7	4231	4231	3161	+ 2
1	112	2829	2829	3169	− 5
1	112	1387	2774	3107	+56
2	198	1593	1593	3154	+ 9
2	198	814.4	1628.8	3225	−62
2	198	538.7	1616.1	3200	−37
2	198	407.4	1629.6	3227	−64
2	99	3255	3255	3223	−60
2	66	4966	4966	3278	−115
3	145	2117	2117	3070	+93
3	145	1100	2200	3190	−27
3	145	545.5	2182	3164	− 1
4	234	1319	1319	3086	+76
4	234	671	1342	3140	+22

$V_R = 3163 \pm 9$ m/sec.

TABLE II. *Velocity of torsional vibrations in thin rods of ice.*

Rod	Wave-length cm	Oscillator frequency cycles/sec.	Rod frequency cycles/sec.	Velocity m/sec.	Residual m/sec.
4	234	823.3	823.3	1926	−13
4	234	409.2	818.4	1915	− 2
4	234	275.6	826.8	1935	+21
4	234	200.9	803.6	1880	+33
4	234	163.3	816.5	1911	+ 3

$V_T = 1914 \pm 6$ m/sec.

By use of the well-known formulas

$$V_R = (E/\rho)^{1/2}, \qquad V_T = (\mu/\rho)^{1/2}$$

we may now obtain all the elastic constants for ice from the observed velocities. Thus, taking $\rho = 0.917$ g/cm³

Young's modulus, $E = 9.17 \pm 0.05 \times 10^{10}$ dynes/cm²
Rigidity, $\mu = 3.36 \pm 0.02 \times 10^{10}$ " "
Bulk modulus, $k = 11.3 \pm 0.6 \times 10^{10}$ " "
Poisson's ratio, $\sigma = 0.365 \pm 0.007$
$\lambda = 9.1 \pm 0.6 \times 10^{10}$ " ".

Direct Measurement of Velocity of Longitudinal Waves in Ice

1. Apparatus and method

The apparatus and method here used were the same which have been used extensively in seismic prospecting. The waves were generated by an electric blasting cap placed in the ice on a lake. An electromagnetic seismograph or geophone was

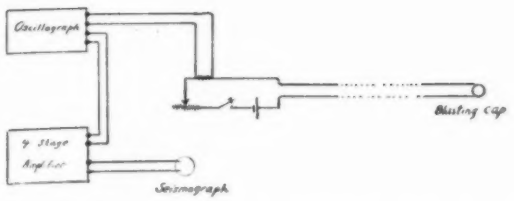

FIG. 2. Schematic diagram of apparatus used in direct measurements of velocity in ice.

placed on the ice in suitable orientation for measuring horizontal motion along the line of travel of the waves. The currents generated by the seismograph were amplified and then recorded in an oscillograph as indicated in Fig. 2. The current through the blasting cap was also registered on the oscillogram and served to determine the instant at which the waves started. Timing marks at intervals of 1/100 second were placed on the oscillogram by means of a tuning fork. Thus the travel time of the vibrations for any desired distance was measured and the velocity was determined. The seismograms obtained at Saylor's Lake are shown in Fig. 3.

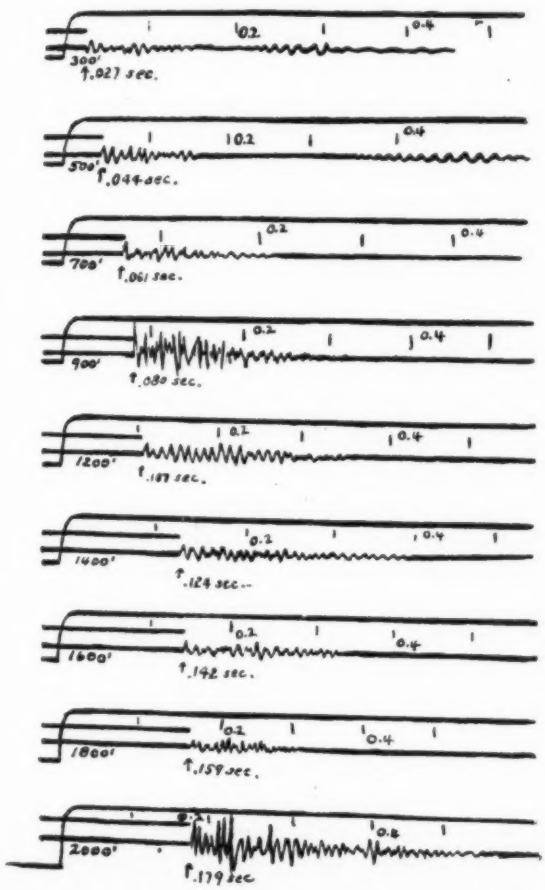

FIG. 3. Seismograms obtained at Saylor's Lake.

2. Results of direct measurement of velocity

One series of measurements was made on Saylor's Lake, a second series on the Lehigh Canal. The data obtained are shown in Tables III and IV, respectively. The values given in these tables for thickness refer to the thickness of the ice sheet at the corresponding firing station. The readings of time from the oscillograms were carried out to the nearest thousandth of a second but the residual errors are practically all less than this amount, indicating a high degree of precision for the measurements. The temperature of the ice was between 0°C and −5°C in each case. Fig. 4 represents the time-distance curves obtained from these data. The fact that this line is straight and passes through the origin is of importance for seismic prospecting. In geologic studies by the seismic method the time-distance curves obtained are seldom straight lines through the origin and it has often been

TABLE III. *Values observed at Saylor's Lake.*

Thickness	Distance	Time	Residual error
4.5 in.	300 ft.	0.027 sec.	−0.0003 sec.
4.5	500	.044	+ .0004
5.0	700	.061	+ .0011
4.5	900	.080	− .0006
4.5	1200	.107	− .0004
4.5	1400	.124	+ .0004
4.2	1600	.142	+ .0001
4.5	1800	.159	+ .0009
4.8	2000	.179	− .0013
	Velocity 11,260±20 ft./sec.		

TABLE IV. *Values observed at Lehigh Canal.*

Thickness	Distance	Time	Residual error
6.0 in.	100 ft.	0.009 sec.	+0.0002 sec.
6.0	200	.019	− .0005
6.0	200	.018	+ .0005
	300	.028	− .0002
7.0	400	.038	− .0010
6.0	500	.046	+ .0002
7.0	600	.055	+ .0005
7.0	700	.065	− .0003
	700	.063	+ .0016
6.0	800	.075	− .0010
	Velocity 10,800±40 ft./sec.		
	Average value of velocity 11,190±30 ft./sec. or 3410±9 m/sec.		

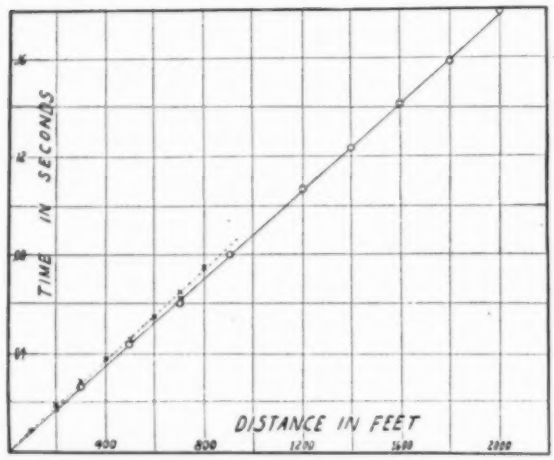

FIG. 4. Time distance curve for longitudinal waves in ice. Circles, Saylor's Lake; Crosses, Lehigh Canal.

argued that some factor such as variation of velocity with amplitude of the disturbance was responsible. The present work proves that those deviations are due to the geologic structure and not to some factor inherent in the seismic method.

Comparison of Results

The velocities V_R, V_P, V_S for longitudinal waves in a thin rod, a thin plate, and in an infinitely extended solid, respectively, are all different. It is well known that

$$V_S = V_R[(1-\sigma)/(1+\sigma)(1-2\sigma)]^{1/2}.$$

Our values for V_R and σ substituted in this formula give 4150 ± 70 m/sec. A value for V_P apparently has not been published. The relation between the strains $\epsilon_1, \epsilon_2, \epsilon_3$ and the stresses p_1, p_2, p_3 are, for an isotropic solid $E\epsilon_1 = p_1 - \sigma(p_2+p_3)$, $E\epsilon_2 = p_2 - \sigma(p_1+p_3)$, $E\epsilon_3 = p_3 - \sigma(p_1+p_2)$. Now, for a plane longitudinal wave in a thin plate we have $p_3 = 0$, $\epsilon_2 = 0$, where ϵ_1 is in the direction of propagation of the wave, ϵ_2 is in the plane of the plate and perpendicular to ϵ_1, ϵ_3 is perpendicular to the plate. Thus

$$p_1/\epsilon_1 = E/(1-\sigma^2)$$

or

$$V_P = [E/\rho(1-\sigma^2)]^{1/2} = V_R/(1-\sigma^2)^{1/2}.$$

Taking the values of $V_R = 3163\pm9$ m/sec. and $\sigma = 0.365\pm0.007$ which were obtained from the measurements of resonance in thin rods of ice the value $V_P = 3400\pm10$ m/sec. which checks nicely with the value

$$V_P = 3410\pm9 \text{ m/sec.}$$

which is the weighted mean of the values obtained by direct measurement at Saylor's Lake and Lehigh Canal.

Correlation of Results with Other Observers

Boyle and Sproule[1] working with longitudinal vibrations of ultrasonic frequencies in thin ice bars, obtained a mean value of 3150 m/sec. for V_R at 0°C. This value checks exceedingly well with our value of 3163 m/sec. at approximately −5°C. Their value of 9×10^{10} dynes/cm² for Young's modulus also checks with our value of 9.17×10^{10} dynes/cm².

In studies on glacier ice by methods similar to our direct method, Mothes,[2] Meisser and Martin, and Sorge[3] obtained for the velocity of longitudinal waves an average value of 3500 m/sec. This value is very much less than our calculated value of longitudinal waves in an infinite solid. If glacier ice is less compact than lake ice this discrepancy may be accounted for. Also since the waves whose velocity was measured, travelled quite near the surface, it is possible the ice did not behave as an infinite solid.

Köhler[4] used a seismic method very similar to our direct method for determining the velocity of waves in lake ice. He obtained a velocity of 3.2 k/sec. for longitudinal and 1.7 k/sec. for transverse waves in ice 30 cm thick. This value for longitudinal waves is in reasonably good agreement with that obtained in the present work, but Köhler did not take account of the fact that the velocity of longitudinal waves is different in a thin plate than in an infinite solid. This oversight makes his values for the elastic moduli of ice unreliable.

Acknowledgments

The explosives used in this experiment were kindly furnished by the Trojan Powder Company. The seismic instruments used were generously donated to the University by the Geophysical Research Corporation.

[1] Boyle and Sproule, Can. J. Research **5**, 601 (1931).
[2] Mothes, Zeits. f. Geophys. **3**, 121 (1927); **5**, 120 (1929).
[3] Sorge, Zeits. f. Geophys. **6**, 22 (1930).
[4] Köhler, Zeits. f. Geophys. **5**, 314 (1929).

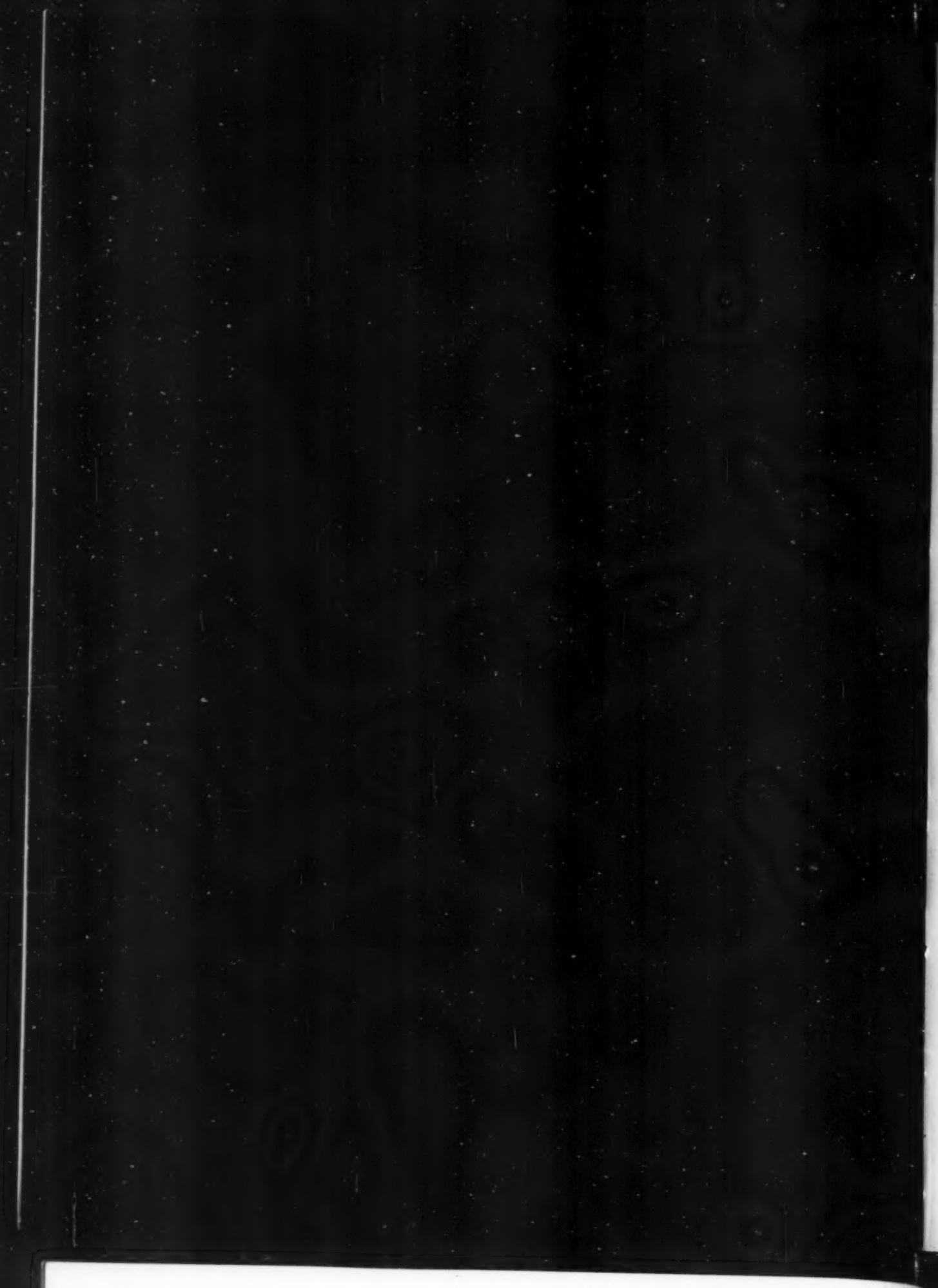

Notice to Contributors

Manuscripts

Send manuscripts to John T. Tate, University of Minnesota, Minneapolis, Minnesota.

Papers must be in English, typewritten double spaced with wide margins.

Abstracts

An abstract must accompany each article. It should be adequate as an *index* and as a *summary*. As an index it should give all subjects, major and minor, concerning which new information is presented. As a summary it should give the conclusions of the article and all numerical results of general interest.

References

References should appear as foot notes, numbered consecutively, and arranged thus:

A. B. Smith, Phys. Rev. **41**, 852 (1932).

Captions and Legends

Legends for figures must accompany manuscript. Each table should have a caption. These in all cases should be complete in themselves so as to make the data intelligible to the reader without reference to the text.

Mathematical Expressions

Make all expressions clear to the typesetter. Identify in the margin of the manuscript Greek letters and unusual symbols.

Use fractional exponents instead of root signs.

Avoid complicated exponents and subscripts. Should it be necessary to repeat a complicated expression a number of times it should be represented by some convenient symbol.

The solidus (/) should be used wherever possible for fractions.

Illustrations

Plan figures for approximately one-half reduction. Wherever possible arrange figures so that after reduction they will not be wider than three inches. Lettering must be large enough to be readable after reduction.

Line drawings must be made with India ink on white paper or tracing cloth. Coordinate paper is not desirable, but if used must be blue-lined and all coordinates to be reproduced drawn with India ink.

Drawings which cannot be used will be returned to the author or redrawn at his expense.

Photographs should show clear black and white contrasts.

Avoid round and oval photographs.

Publication Charge

A portion of the cost of publishing the results of research must be regarded as an integral part of the cost of the research. In keeping with the policy which is effective for the Institute's publications a bill for $3.00 per page will be sent to the authors of papers appearing in this journal. It is intended that the authors shall present these bills for payment to the institutions which have supported their researches. If the institution is unable to make payment the bills are to be returned marked "No Funds Available."

Reprints

As a partial return for the publication charge one hundred reprints without covers will be furnished free. Additional reprints may be obtained at a regular schedule of prices.

Alterations

Take great care that each manuscript is typographically accurate. A limited number of alterations in proof are unavoidable, but the cost of making extensive alterations after the article has been set in type will be charged to the author.

Proof and all correspondence concerning papers in the process of publication should be addressed to the Editorial Secretary, American Institute of Physics, 11 East 38th Street, New York, N. Y.

THE AMERICAN PHYSICAL SOCIETY

ARTHUR H. COMPTON, *President*
University of Chicago
Chicago, Illinois

R. W. WOOD, *Vice-President*
The Johns Hopkins University
Baltimore, Maryland

W. L. SEVERINGHAUS, *Secretary*
Columbia University
New York, New York

G. B. PEGRAM, *Treasurer*
Columbia University
New York, New York

JOHN T. TATE, *Editor*
University of Minnesota
Minneapolis, Minnesota

L. B. LOEB, *Local Secretary for the Pacific Coast*
University of California
Berkeley, California

THE object of the American Physical Society is the advancement and diffusion of the knowledge of physics. It sponsors *The Physical Review*, *Physics* and the *Reviews of Modern Physics*. Upon the recommendation of two or more members, any person engaged in work in the field of physics or actively interested in physics may become a member; receive one of the journals; receive also *Science Abstracts* A, *The Review of Scientific Instruments with Physics News and Views*, and the Bulletin of all meetings; and attend and participate in the seven annual meetings.

Annual dues: $10. Fellows, $14.

For further information address the Secretary as above.

THE SOCIETY OF RHEOLOGY

S. E. SHEPPARD, *President*
Eastman Kodak Company
Rochester, New York

EUGENE C. BINGHAM, *Editor*
Lafayette College
Easton, Pennsylvania

A. STUART HUNTER, *Secretary & Treasurer*
Du Pont Rayon Company
Buffalo, New York

THE Society of Rheology was formed in 1929 to advance the science of the deformation and flow of matter. It cooperates with the American Physical Society in editing *Physics* of which four issues per year are devoted to *Rheology*. All persons interested are invited to become members and participate in the proceedings at the annual December meetings. Members receive without other charge than their dues all issues of *Physics*, *The Review of Scientific Instruments with Physics News and Views* and the notices of the Society.

Annual dues: $6.

For further information address the Secretary as above.